Available online at www.sciencedirect.com

ScienceDirect

Procedia Engineering 213 (2018) 79–88

Procedia Engineering

www.elsevier.com/locate/procedia

7th International Conference on Fatigue Design, Fatigue Design 2017, 29-30 November 2017, Senlis, France

# Fatigue resistance of selectively laser melted aluminum alloy under T6 heat treatment

Julius N. Domfang Ngnekou[a,b]*, Gilbert Henaff[a], Yves Nadot[a],Julien Nicolai[a], Lionel Ridosz[b]

[a]*Institut Pprime UPR CNRS 3346, Department of Physique and Mechanics of Materials, ENSMA-Université de Poitiers, 1 avenue Clément Ader, Téléport 2, 86960 Chasseneuil-Futuroscope, France*
*bZodiac Aerospace, 61 rue Pierre Curie, 78370 Plaisir, France.*

**Abstract**

Due to complex microstructure and defect inherited from this ALM process, it is necessary to assess the fatigue resistance of the material constitutive of manufactured parts prior to certification. This work is precisely tackling this issue with a special attention paid to the role of microstructural parameters and defects on fatigue life. Specimens were built with two configurations (0° and 90°) in order to evaluate the impact of the induced anisotropy of microstructure on fatigue properties. X-Ray 3D tomography was used to characterize defect population by their size. Microstructure is furthermore characterized by considering four characteristic scales **[1-3]**: melt-pools, crystallographic grains, dendritic structure and the precipitates. The fatigue properties are determined by establishing S-N curves for as-built and heat-treated samples for R= -1. The defect size responsible for the fatigue damage initiation is determined in each sample so as to establish a relation between the fatigue limit and the defect size by means of Kitagawa type diagrams. It is shown that the defect size is the first order parameter in terms of the fatigue resistance. Through the Kitagawa diagrams for as-built and heat treated samples, we quantify the improvement of the fatigue resistance due to the peak hardening treatment.


Peer-review under responsibility of the scientific committee of the 7th International Conference on Fatigue Design.

* Corresponding author.
*E-mail address:* julius.domfang@ensma.fr

1877-7058 
Peer-review under responsibility of the scientific committee of the 7th International Conference on Fatigue Design.
10.1016/j.proeng.2018.02.009

**Nomenclature**

| | |
|---|---|
| UTS | Ultimate Tensile Stress (MPa) |
| YS | Yield Stress (MPa) |
| Ef | Elongation to failure (%) |
| Ra | Arithmetic roughness (µm) |
| W | mass composition (%) |
| DAS | Dendritic Arm Spacing (µm) |
| SDAS | Secondary Dendritic Arm Spacing (µm) |
| A | Basquin coefficient |
| $\sigma_{D-1}^{ta}$ | Fatigue limit for alternating tension at R=-1 |
| $N_f$ | Number of cycle at failure |
| $\sigma_n$ | Stress amplitude at step n |
| $\sigma_{n-1}$ | The stress amplitude at step n-1 |
| $\sigma_{max}$ | Maximum stress in load direction |

*Keywords:* Fatigue, Defect size, AlSi10Mg, ALM, Microstructure, T6.

## 1. Introduction

Additive manufacture is considered to be a process that breaks with the existing ones, insofar as it offers, in particular, the possibility of producing parts with complex geometry and topographically optimized. In the aeronautical context, the realization of the parts involves them qualification which means the understanding of the fatigue behavior due to integrity of the material. So, the knowledge of the microstructure of the material so as the metallurgical defects inherited to the manufacturing process is therefore necessary in order to quantify the impact of each material parameter on the fatigue behavior of such parts. Thus it will be possible to tend towards the optimization of the process regarding the fatigue behavior. In this work, we are talking about a hypo eutectic aluminum alloy developed by the ALM process. Some studies have been carried out on the microstructural characterization and defects, as well as the anisotropy effects due to the direction of growth of the specimens in relation to the statics mechanical properties such as UTS, Ys and Ef **[3, 4].** Concerning the fatigue, Brandl et al [**5]** showed that anisotropy due direction of production is observable for the platform temperature of 30 ° C. According to the previous author by coupling a platform temperature of 300°C and a T6 heat treatment, no difference is visible anymore due to the direction of sample growth. Maskery et al **[6]** evaluated the impact of T6 treatment on fatigue performance for as built manufacturing surfaces; they work showed a significant increase in the fatigue limit due to T6 treatment. According to Aboulkhair et al **[7]**, the specimens machined from the T6 heat treated bars have a greater fatigue resistance. Few studies quantify the impact of defects on the fatigue limit. This study proposes to evaluate through the Kitagawa type diagrams the impact of defects size on the fatigue limit with and without T6.

## 2. Experimental approach

### 2.1. Material and samples

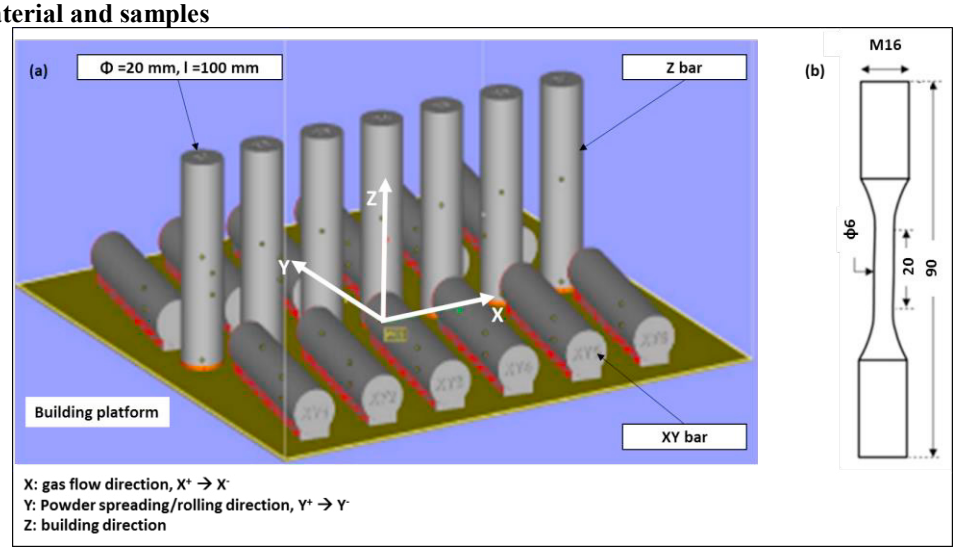


*Figure 1: (a) Position and orientation of bar, (b) machined fatigue test specimen*

Two distinct productions of AlSi10MgSi by SLM, noticed P1 and P2, were considered in the present study.
Firstly, a PHENIX PM100 developed by 3D SYSTEMS was used for the P1 production using TLS powder. This machine is equipped with a 200W fiber laser YAG. The layering is done by means of a roller. All P1 specimens have been removed from XY bars built on an aluminum platform at 200°C. In order to relax the stress due to the process, a post processing heat treatment have been performed during one hour at 160°C. The P1 specimens were tested on a rotative bending machine. The results of the P1 production tests were analyzed and used as a reference for the study. Secondly, the P2 samples were built on a platform at 200°C using EOS M290 machine and EOS powder. This machined is equipped with a 400 W fiber laser, and the layering is performed by means of a scraper. A stress relaxation treatment have been performed during 2 hours at 300°C. Both powders used for P1 and P2 have chemical compositions in accordance with standard NF EN 1706:2010. P2 samples have been built in two directions, namely XY and Z as in ***figure 1-a***. Fatigue specimens test have been machined (MA) from the produced bars by fine turning. Fatigue test specimens geometry is given on ***figure 1-b***. After machining, some specimens have been subjected to heat treatment T6 with specific conditions in ***table 1***. As it is shown on ***table 2***, and depending on production number, orientation and T6 or not, different designation for fatigue specimen is used in this paper.

*Table 1: conditions du T6*

| Steps | Temperature (°C) | Duration (h) | Environnement |
|---|---|---|---|
| Solid solutioning | 540 | 8 | Air |
| Quenching | 20 | | Water |
| Tempering 1 | 20 | 24 | Air |
| Tempering 2 | 160 | 10 | Air |
| Cooling to room temperature | | | |

*Table 2: material designation*

| Production | Orientation | Treatment | Designation |
|---|---|---|---|
| P1 | XY | Without | P1-XY-MA |
| P2 | XY | Without | P2-XY-MA |
| | | T6 | P2-XY-MA-T6 |

| | | | |
|---|---|---|---|
| | Z | Without | P1-Z-MA |
| | | T6 | P2-Z-MA-T6 |

### 2.2. Microstructure characterization

Before studying the microstructure, the different element present in the alloy have been quantified using EDX measurements. As reported in ***table 3*** the composition determined is in accordance with the standards. However, the non-detection of some elements such as iron for example does not mean that it is absent in the matrix but that it is present in a small proportion, and distributed homogeneously in the volume; so that it cannot be detected by the EDX technique.

*Table 3: chemical composition of the alloy*

| | Al | Si | Fe | Cu | Mg | Mn | Zn | Ti |
|---|---|---|---|---|---|---|---|---|
| NF EN 1706:2010 | Bal. | 9-11 | <0.55 | <0.05 | 0.2-0.45 | <0.45 | <0.1 | <0.15 |
| W% EDX measure | Bal. | 9.55 | | | 0.4 | | | |

In order to characterize the microstructure due to the ALM process specimens were machined from the center of cylindrical bars.

This investigation leads to a description of the microstructure along four main characteristics parameters, namely:

- The melt-pools that can be geometrically characterized by them length, width and height, and which reflect the impression left by the laser during the melting of the deposed powder. As shown in ***figure2-a***, these melt-pools are strongly anisotropic in shape. Measurements of the melt-pool dimensions have been performed on those melt-pools by images analysis and the mean values are (600; 150; 80) corresponding to (length, width and height). A fine study of the interior and of the boundaries of the melt-pools by Kempen et al **[1]** has shown that those melt-pools are constituted of the heterogeneous distribution of eutectic silicon in the alpha-phase aluminum. In ***figure2-b*** it can further be noticed that, after heat treatment, the melt-pool boundaries are no longer visible, presumably due to the diffusion and dissolution of the silicon in the aluminum matrix. According to Li et al **[2],** the higher the solution temperature, the coarser are the silicon particles typically around 2 to 4 µm within a range of 450°C to 550°C. Additional growth of these particles is achieved during artificial aging.

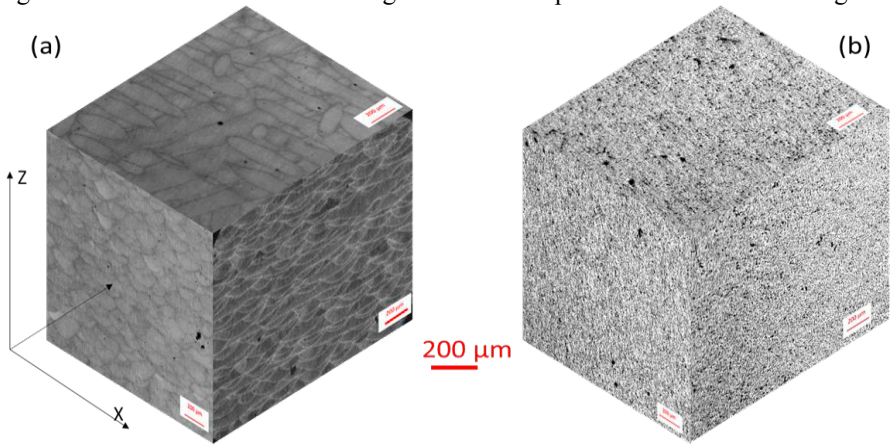


*Figure 2: 3D reconstructions of optical microscopy observations of the microstructures after surface polishing, without etching, (a): without heat treatment (b): after T6*

- The dendritic structure is geometrically characterized by the diameter of the eutectic silicon observed from the scanning plan, and by the distance between two fibrous eutectic silicon seen from transversal plans. The rapid solidification involved in SLM process does not allow the formation of the dendritic structure with secondary arms as it is the case for cast aluminum alloy **[8]**. Therefore, in this study, a Dendritic Arm Spacing DAS

dimension of about 0.5 to 2 µm was determined, which is significantly smaler compared to the characteristic SDAS parameter in cast aluminum alloys (30 to 100µm function of cooling rate). Previous studies have shown that this parameter has a large influence on the fatigue behavior **[8, 9]**. Typically, according to Wang et al **[9,]** in absence of defect, the finer the SDAS, the higher is fatigue life. As previously mentioned, the melt-pools are decorated by eutectic phases. Many studies **[1, 2, 11]** agree on the point that this silicon distribution reveals the dendritic structure of the alloy.

- Crystallographic grain orientations have not been characterized using EBSD technique. However, according to Lore et al **[1],** grains are strongly anisotropic in term of geometry and textured with an epitaxial growth. It is also important to mention that the grain growth can encompass one to three melt pools, reflecting the size of powder bed. According to Wang et al **[10]**, the peak hardening treatment does not affect the size and shape of grains. Therefore, in this study we will consider that the grains are not affected after T6 treatment.
- Silicon precipitates and iron rich needles mostly appears after T6. In fact, during the heat treatment, diffusion and segregation of Si and Fe atoms occurs, leading to the formation of Fe-rich precipitates and Si crystals randomly distributed in the Al-matrix. A quantitative study of precipitates have been performed on a thin foil removed from a heat treated samples by FIB milling. TEM analysis of this foil shows the presence of twinned silicon grains with 98% of silicon for only 2% of aluminum, Fe-rich (10/41/49 - Fe / Al / Si) needles, mostly β-Al7FeSi2 and β-Al6Fe2Si2 compounds, and large mono-crystalline aluminum grains oriented along [112] and [114] directions.

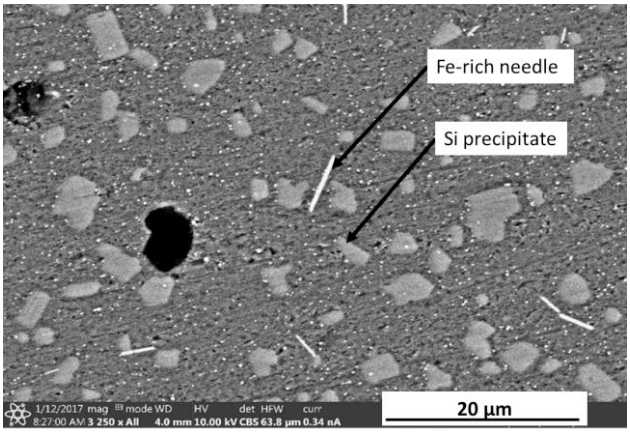


*Figure 3: SEM (SEI) observation of the T6 microstructure (polish, without etching): precipitation structure and intermetallics needles*

### 2.3. Defect characterization in relation with the process parameters

Different techniques can be carry out to characterize the defects in a sample in terms of defect type, size, morphology and location. Firstly, it is possible to use optical microscope on a cross section previously polished. However this method can bring several errors induced by the preparation of samples, especially cutting and polishing. An alternative method could consist in observing a fracture surface after completion of a fatigue test for example. The principal advantage of this method lies on the fact that the critical defect and its location are a posteriori determined. By observing fracture surfaces such as in ***figure 6***, two main families of defects inherited to SLM process are evidenced:

- The gas pores, characterized by a spherical shape. These defects are due to the interaction between the laser beam and the powder bed, especially for high laser power and low scanning speed.
- The unmelted particles and/or lack of fusion characterized by a complex geometry. Those defects are mainly related ue to the layering process and also to the projection of molten metal droplets onto the powder bed. The droplets then covers unmelted particles and increases the energy required to melt them as the unmelted particles below.

However the observation of a fracture surface means the lost of a lot information about the critical defect. Thus, a deterministic method is required to collect all information on a given defect present in a given specimen. As a consequence, the X-ray tomography have been used here. .

In this technique, the specimen is fixed to a rotating support and it is then subjected to an X-ray beam. A screen

collects the more or less attenuated signal in relation with the local permeability of the material. Several images are then taken where it is possible to observe a contrast and brightness corresponding to the presence or absence of defects. By After a post-treatment using Avizo® software package, all images are binarized and a segmentation is done so that it is possible to reconstitute defects as ***figure 4-a***. As shown in ***figure 4-b***, the defect size distribution lies the 28 to 52 µm range. As it can be seen on fracture surface, the fatal fatigue crack is due to a defect that is clearly the bigger contained by the samples. Which means the fatigue is not sensitive to all the defect population but to the bigger one.

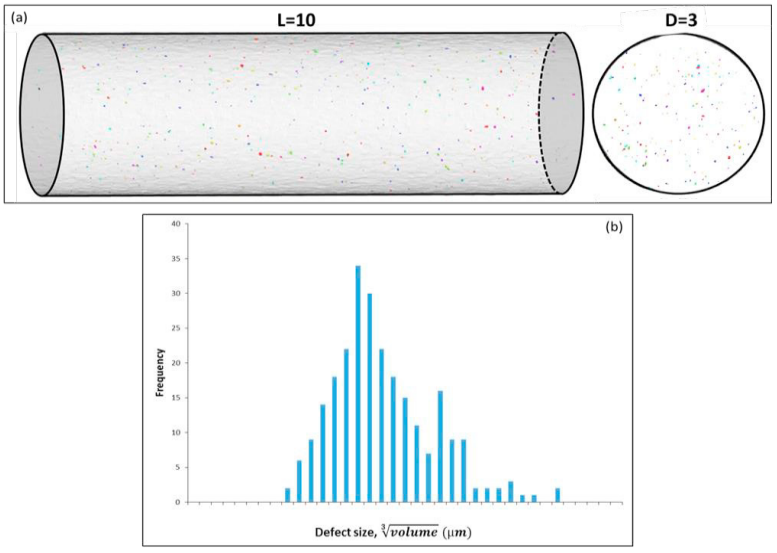


*Figure 4: (a) Characterization of the defect induced by the SLM process, using X-ray tomography with a resolution of 5µm per voxel (b) defect size distribution*

### 2.4. Fatigue test

In this study cylindrical specimens were used as shown on ***figure 1-c***. Fatigue tests have been performed at room temperature on resonance machine with a load ratio R=-1. The frequency was in the range of 80 to 82 Hz.

### 2.5. Determination of the fatigue limit

The fatigue limit have been defined at one million cycles. A step by step method described by Iben Houria **[12]** have been used as it is the only way to evaluate the fatigue limit for a natural defect. It is assumed that no significant damage is introduced in the loading as shown by Roy et al [**13]** for cast alloy A356. The failure is define by a 5Hz drop of frequency. The fatigue limit is then determined for each specimen after failure according to the following method:

- When a specimen fails during a first step, a Basquin equation is used to calculate the fatigue limit.

$$\sigma_{D-1}^{ta} = A * N_f^{\alpha}$$

  Where A and α are constants determined from experimental results.

- When the specimen fails after one or several steps, the fatigue limit is determined by a linear interpolation according to the following equation:

$$\sigma_{D-1}^{ta} = \frac{N_f}{10^6} * (\sigma_n - \sigma_{n-1}) + \sigma_{n-1}$$

Where $\sigma_{D-1}^{ta}$ is the fatigue limit for alternating tension at R=-1 ratio, $\sigma_{n-1}$ the stress amplitude at the n-1 step, and $N_f$ the number of cycle at failure.

## 3. Results and discussions

The analysis of the fatigue test is focused on the anisotropic effects due to the process. The effect of anisotropy induced by the building strategy (XY versus Z) will be examined on the basis of S-N curves for machined and machined plus T6. Secondly, for same samples configurations, Kitagawa-type diagrams are considered to quantify the effect of defect size on fatigue limit.

### 3.1. S-N curves

Even though the microstructure is strongly anisotropic in non-heat-treated samples, no difference is noticed between XY and Z samples in terms of fatigue life. The Basquin curves indicate a slight anisotropy effect between XY and Z samples. On the ***figure 5*** the S-N curves of P2 machined and heat treated samples are compared. The fatigue limit is estimated using an extrapolation with least square method. A 20% augmentation in fatigue limit is observed between P2-XY-MA and P2-XY-MA-T6 while more than 45% is observed for Z samples. Compared to P1-XY-MA the fatigue limit at one million of cycle of P2-XY-MA is improved by about40%. The fracture surface examination in ***figure 6*** furthermore suggests that a significant increase of fatigue limit between P1 and P2 is primarily due to a reduction in the critical defect size. For all P2 specimen containing similar defects, an increase of fatigue limit is noticed after T6 despite the presence of iron needles which are supposed to degrade the fatigue crack initiation tolerance **[14]**. That increase observed after heat treatment is due to the strengthening of the matrix via the applied T6. However it is observed that a peak hardening treatment leads to a more pronounced anisotropy effect between XY and Z orientations.

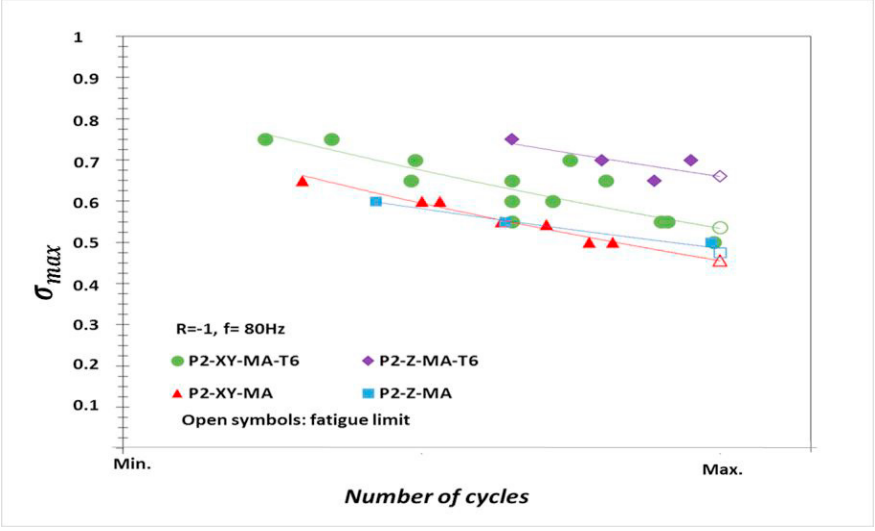


*Figure 5: effect of building direction on fatigue life for as-built and T6 samples.*

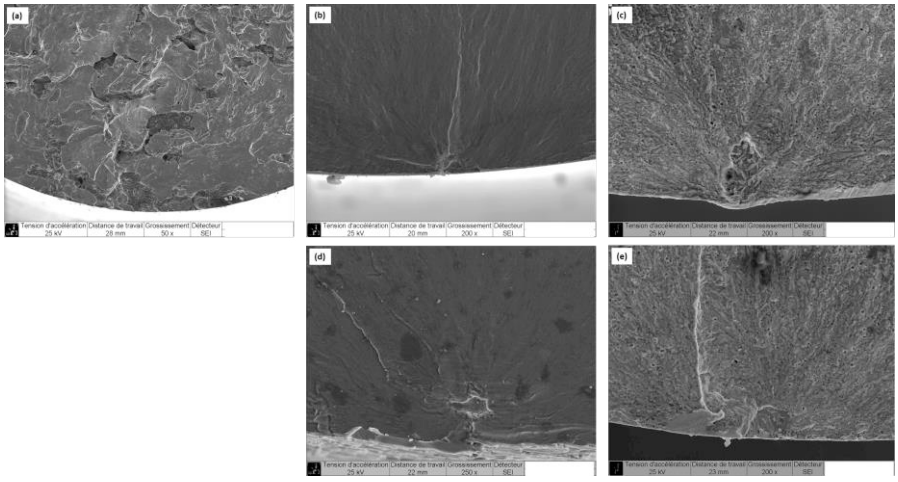


*Figure 6: priming sites (a) P1-XY-MA (b,d) P2-XY and Z –MA (c,e): P2: XY and Z-MA-T6*

### 3.2. Kitagawa diagram

The examination of the fracture surfaces indicates that the fatigue failure is mostly controlled by initiation on metallurgical defects inherited from the ALM process. In order to plot the Kitagawa type diagram, defect size

have been assessed using Murakami's parameter $\sqrt{area}$ . Moreover ***Figure 7*** explains the criterion used to define the defect size according to **[15].** In ***figure 8*** the fatigue limit is plotted as a function of the defect size measured on fracture surfaces. In order to extend the range of this study, spherical artificial defects were introduced by electro discharge machining (EDM). For both types of microstructure, i. e. none and peak-hardened, even in presence of defects, the Kitagawa-type diagram shows that the fatigue limit is sensitive to defect size; it also confirms the observation on anisotropy made on S-N curves. For P2-XY/Z-MA the fatigue limit is controlled by the defect size beyond a certain defect size while in the T6 microstructure, the concept of defect free material seems not yet acquired. As a consequence under a critical defect size the fatigue life is controlled by the precipitation structure and the defects. Furthermore, ***figure 8*** shows there is no influence of defect type and all the trends curves seems to converge for big defect.

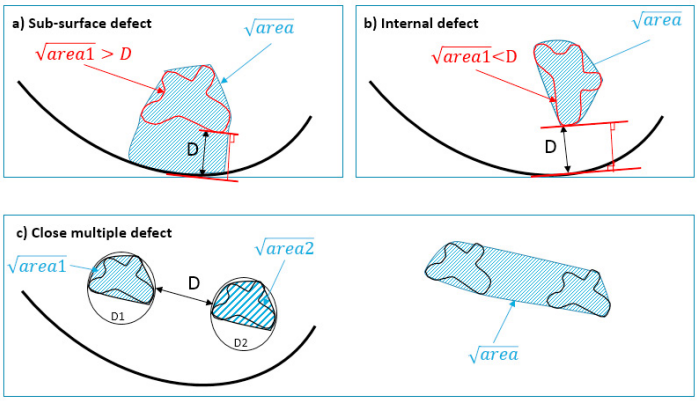


*Figure 7: assumption for the assessment of the defect size*

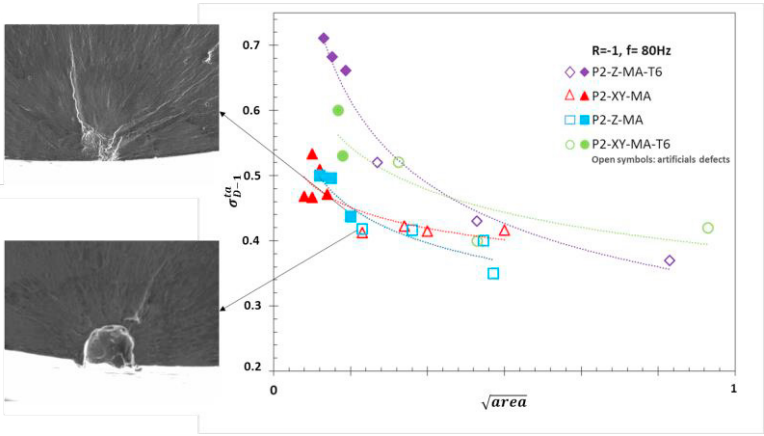


*Figure 8: Kitagawa type diagram for MA and MA-T6 specimens*

## 4. Conclusions

In this study, AlSi10Mg material have been characterized before and after T6 using five mains scales:

- Melt-pools (600x150x80 µm3), which disappear after T6;
- The cells-α or DAS (0.5 to 2 µm);
- Crystallographic grains;
- The precipitation structure:
  - The precipitates of silicon (4 to 10 µm), more numerous after T6;
  - The FeSi needles, which appear after T6;
- Defects inherited to the process

In order to understand the role of the microstructure on fatigue behavior, the fatigue limit have been quantified. This

led to the following fatigue results:

- For the same defect size for non-heated material, there is no anisotropy effect due to the direction of production;
- In presence of defects, improvement of the matrix via the T6 heat treatment improves fatigue strength;
- An isotropy between XY-MA-T6 and Z-MA-T6 is observed.

The impact of defect size have been quantify Through the Kitagawa type diagrams. It was observed that:

- There is no influence of the defect type on the fatigue limit;
- The critical defect size due to the process have been quantify;
- It exist a value of defect size beyound that the fatigue limit is controlled only by the defect size, below that size, the fatigue limit is controlled by the defect size and the microstructure.

## 5. Acknowledgement

The authors gratefully acknowledges funding provided by Zodiac Aerospace and French National Research and Technology Association (ANRT). This work was partially funded by the French Government program “Investissements d'Avenir” (EQUIPEX GAP, reference ANR-11-EQPX-0018). This work partially pertains to the French Government program "Investissements d'Avenir" (LABEX INTERACTIFS, reference ANR-11-LABX-0017-01).This work has been partially supported by « Nouvelle Aquitaine » Region and by European Structural and Investment Funds (ERDF reference: P-2016-BAFE-94/95).Thanks to Thierry ROUGE-CARRASSAT for his fruitful comments on the manuscript.

## 6. References

[1]: L. Thijs, K. Kempen, J.P. Kruth, J. V. Humbececk, Fine-structured aluminium products with controllable texture
by selective laser melting of pre-alloyed AlSi10Mg powder, Acta Materialia 61(2013) 1809-1819

[2]: Wei Li, Shua Li, Jie Liu, AngZhang, Yan Zhou, Qingsong Wei, Chunze Yan, Yusheng Shi, Effect of heat treatment on AlSi10Mg alloy fabricated by selective laser melting: Microstructure evolution, mechanical properties and fracture mechanism, Material Science & Engineering A 663 (2016) 116-125

[3]: Nesma T. Aboulkhair, Ian Maskery, Chris Tuck, Ian Ashcroft, Nicola M. Everitt, The microstructure and mechanical properties of selectively laser melted AlSi10Mg: the effect of a conventional T6-like heat treatment, Material Science & Engineering A 663 (2016) 139-146

[4]: K. Kempen, L.Thijs, J. Van Humbeeck and J.-P. Kruth, Mechanical properties of AlSi10Mg produced by Selective Laser Melting, Physics Procedia 39 ( 2012 ) 439 – 446

[5]: Erhard Brandle, Ulrike Heckenberger, Virtus Holzinger, Damien Buchbinder, Additive manufactured AlSi10Mg samples using Selective Laser Melting (SLM): Microstructure, high cycle fatigue, and fracture behavior, Material and Design 34 (2012) 159-169

[6]: I. Maskery, N. T. Aboulkhair, C. Truck R.D. Wildman, Fatigue performance enhancement of selective laser melted aluminium alloy by heat treatment

[7]: Nesma T. Aboulkhair, Ian Maskery, Chris Tuck, Ian Ashcroft, Nicola M. Everitt, Improving the fatigue behaviour of a selectively laser melted aluminium alloy: Influence of heat treatment and surface quality, Material and Design 104 (2016) 174-182

[8]: Mohamed Iben Houria, Yves Nadot, Raouf Fathallah, Matthew Roy, Daan M. Maijer, Influence of casting defect and SDAS on the multiaxial fatigue behaviour
of A356-T6 alloy including mean stress effect, International Journal of Fatigue 80 (2015) 90–102

[9]: Q.G. Wang *, D. Apelian, D.A. Lados, Fatigue behavior of A356-T6 aluminum cast alloys. Part I. Effect of casting defects, Journal of Light Metals 1 (2001) 73-84

[10]: JIANG Wen-ming, FAN Zi-tian, LIU De-jun, Microstructure, tensile properties and fractography of A356 alloy under as-cast and T6 obtained with expendable pattern shell casting process, Trans. Nonferrous Met. Soc. China 22(2012) s7−s13

[11]: Tang Ming, Inclusion, porosity, and Fatigue of AlSi10Mg Parts Produced by Selective Laser Melting (2017) Dissertation. 903

[12]: Mohamed Iben Houria, Experimental investigation and modeling the fatigue life of a cast aluminium alloy A356-T6 under multiaxial loading (2015) Dissertation

[13]: M. Roy, Y. Nadot, C. Nadot-Martin, P.-G. Bardin, and D. Maijer, "Multiaxial Kitagawa analysis of A356-T6,"

*International Journal of Fatigue,* vol. 33, pp. 823-832, 2011.
[14]: J. Yi, Y. Gao, P. Lee, and T. Lindley, "Effect of Fe-content on fatigue crack initiation and propagation in a cast aluminum–silicon alloy (A356–T6)," *Materials Science and Engineering: A,* vol. 386, pp. 396-407, 2004.
[15]: Y. Murakami and M. Endo, "Effects of defects, inclusions and inhomogeneities on fatigue strength," *International Journal of Fatigue,* vol. 16, pp. 163-182, 1994.